CIRP Annals - Manufacturing Technology 00 (2022) 1–4

Contents lists available at ScienceDirect

CIRP Annals - Manufacturing Technology

journal homepage: https://www.editorialmanager.com/CIRP/default.aspx

Inducing <111> texture in AA5182-O through continuous-bending-under-tension and recovery heat treatment processes to influence r-values

Jinjin Ha, Sarah Mayer, Zhangxi Feng, Nikolai Matukhno, Marko Knezevic, Brad L. Kinsey (2)*

Department of Mechanical Engineering, University of New Hampshire, Durham, NH, USA

ARTICLE INFO

Article history:
Available online xxx

Keywords:
Texture
Heat treatment
Stress superposition

ABSTRACT

Crystallographic texture in metals influences material properties, e.g., r-value. In this work, a moderately strong <111> texture is obtained in AA5182-O through continuous-bending-under-tension processing followed by a recovery heat treatment from the initial weak cube <001> texture. EBSD scans confirm that the <111> texture is retained after heat treating. The processed material exhibits increased strength and reduced planar anisotropy, providing benefits to subsequent forming operations, compared to the as-received material. Crystal plasticity simulations confirm the texture change during deformation and predict the flow stress response. Such simulations can be used for stress superposition process design to intentionally manipulate material properties.

1. Introduction

The crystallographic texture of metallic materials has a significant effect on the material behavior, e.g., yield stress, ductility, plastic anisotropy, stress-strain response, failure, etc. For example, strong texture of <111> and <012> fiber created by hot rolling in AA6013 at 400 °C induces strength increase without compensating the achievable total elongation [1]. Varying loading paths in the process also affects the texture induced, potentially with an interaction of other microstructural features like twinning/detwinning, such as under tension, compression [2], equibiaxial [3], torsion, etc.

Although initial examples of such efforts date back to the 1960′s without specifying the overarching effect [4], a relatively new concept with respect to manipulating the loading to achieve improvements in forming processes is stress superposition [5]. This is defined as the introduction of additional stresses to a primary forming operation in a single process step. Stress superposition can be used to lower the forming forces in a process. For example, Roskosz et al. showed that the required compression load of sintered steel specimens was decreased when a reciprocating torsional load was simultaneously applied [6]. Alternatively, stress superposition can be used to improve the formability of the material in an operation to achieve a strain value or geometry not possible with typical loads applied. For example, a lateral extrusion process of AA7075 into a four-legged component was only feasible without cracking if a compressive load was applied to the four legs during the process [7]. An emerging concept in stress superposition is to employ such loading strategies to affect material properties of final parts. For example, during incremental forming, the residual stress in the part wall can be varied by forming with or without an elastomer die, which applies an additional compressive force, in the process [8]. Another example of localized stress superposition, which has been shown to reduce forming forces and prevent the localization of deformation that leads to fracture, is continuous-bending-under-tension (CBT) processing of material [9].

In CBT, the material is pulled in tension while simultaneously being passed through rollers, which have, e.g., diameters (D), are set a distance (L) apart, and have a specified bending depth (δ). In addition to these parameters, the pulling speed of the applied tension (v) affects the CBT process results. See Fig. 1 for a schematic of the process. Specifically, CBT has been shown to reduce the forming loads of DC04 by approximately 40% [9]. With respect to increasing the deformation possible, the elongation to fracture of a DP1180 was increased by five-fold through CBT processing [10]. However, the residual stress and increased dislocation density developed during CBT processing depletes the potential elongation during subsequent forming operations and raises the stress required to continue deformation [11]. Thus, an appropriate heat treatment for recovery should be implemented with CBT as a pre-processing step prior to forming to maintain the benefit of enhanced formability through the process, e.g., deep drawing. CBT processing has also been shown to induce a fiber <111> texture, which enhances the material formability relative to the cube-dominated texture in rolled FCC materials, throughout the gauge length of a CBT specimen with a comparable intensity [12]. This texture is present in the fracture region in a uniaxial tension test. However, whether this texture can be induced and then sustained through recovery heat treatment and the effect on the final material properties has not been investigated in past research.

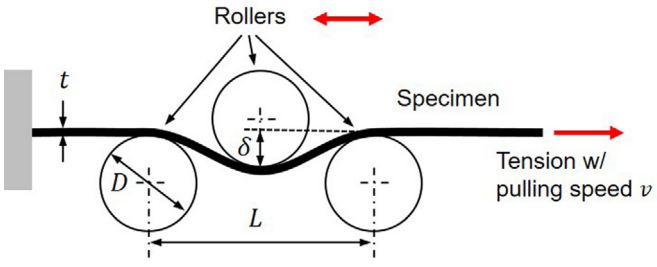

Fig. 1. Schematic of continuous-bending-under-tension process.

In this paper, a typical cube <001> texture of AA5182-O in the as-received condition is altered to a fiber <111> texture through CBT processing. As the potential elongation is depleted, further elongation prior to fracture is regained through a recovery heat treatment, while avoiding recrystallization of the material. Textures in all of these conditions are observed through electron beam

* Corresponding author.
E-mail address: bkinsey@unh.edu (B.L. Kinsey).

https://doi.org/10.1016/j.cirp.2022.04.059
0007-8506/

backscatter diffraction (EBSD). Subsequent uniaxial tension tests using subsized tensile specimens are performed to measure the stress-strain response of the material conditions. The r-value, i.e., width to thickness plastic strain increments ratio, during the tests is obtained to evaluate the plastic anisotropy of the material in the rolling (RD), diagonal (45°), and transverse directions (TD). Elasto-plastic self-consistent (EPSC) simulations are employed to further study and in the future exploit the effects observed. This work is an example of using stress superposition, i.e., combined tension and bending loading in the CBT process, to intentionally manipulate final properties of the material.

2. Experimental processing

Strips of AA5182-O are CBT processed per the details provided below and then a recovery heat treatment is conducted. Various temperatures and times are evaluated for this recovery process. The ones that provided the best results are presented. While only a strip type of specimen is investigated for this research, the concept could be applied to sheets of material in the regular rolling process sequence as the material is leveled, a process similar to CBT but with less severe deformation, and annealed already between rolling operations.

2.1. Continuous-bending-under-tension (CBT) process

The experiment is performed using a custom CBT machine built at the University of New Hampshire (UNH) [10–14], which is based on the same concept as Fig. 1. A picture of the UNH CBT machine is shown in Fig. 2 with detailed components of a moving carriage via a ball screw mechanism, two stationary stands assembled with three rollers, a base, a hydraulic cylinder, and data acquisition and control systems labeled. The best CBT processing conditions of bending depth, δ =3 mm, and crosshead velocity, v = 1.3 mm/s, are determined based on when the maximum displacement to fracture, which is equivalently the maximum number of CBT cycles, is achieved. The carriage moving velocity is 66 mm/s.

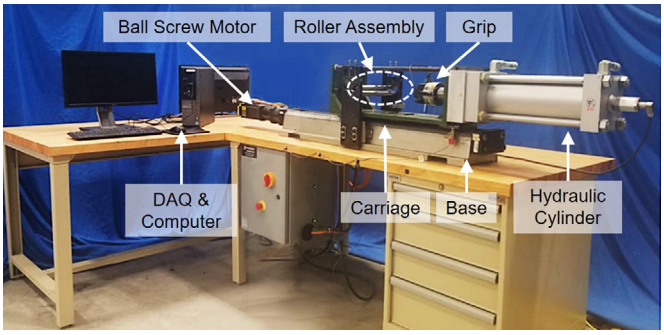

Fig. 2. Experimental setup for CBT processing with UNH machine.

Fig. 3 shows the force-displacement curves from CBT processing with the predefined parameters for δ and v and simple tension without any bending effect. It should be noted that both tests use the same geometry of CBT specimen. Repeated peaks, which occur in the CBT force-displacement curve, i.e., 15 sets of peaks in Fig. 3, indicate the number of CBT cycles and instances when the rollers are locating at each specimen end and the carriage stops to switch directions. This causes an abrupt increase in the force as the deformation is momentarily simple tension without bending. (For further explanation of the CBT force-displacement curve, please see [13].) From the comparison with the simple tension, the CBT processing exhibits three times greater maximum displacement achievable with almost half of the processing force during the deformation with the given CBT parameters. The thickness after CBT is decreased from 1.55 mm to 1.13 mm, resulting in 27.1% thickness reduction.

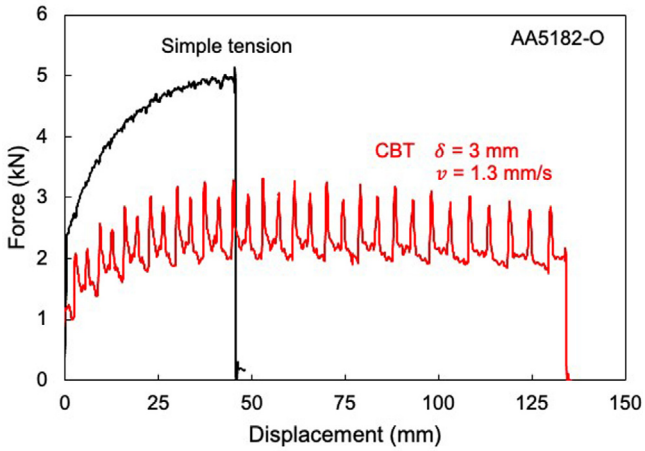

Fig. 3. Force-displacement curves for CBT processing (red) and simple tension (black) with the same tension velocity. Specimen is along the RD.

2.2. Recovery heat treatment

CBT processing induces undesirable microstructure changes, such as residual stresses and dislocations, which must be addressed if CBT processed material is to be used in subsequent forming operations. Heat treatment can resolve this issue but should avoid grain recrystallization to maintain the <111> texture induced by the CBT processing. Two hours of heat treatment at 270 °C are identified as the best heat treatment conditions for recovery among five temperatures (220, 250, 260, 270, and 280 °C) and four times (0.5, 2, 3, and 4 h) investigated. EBSD scans along with stress-strain curves confirm the maximum recovery without any, or at least very few, recrystallized grains and partial recovered potential elongation, respectively. Heat treatment is performed using a Carbolite Gero GPCMA/37 oven with a 3504 controller. The oven is heated to the specified temperature before the specimen is placed inside. The specimen temperature is also tracked using a K-type thermocouple. Specimens are air cooled after the recovery heat treatment.

3. Material characterization

The effect of the CBT processing and recovery heat treatment on the microstructure and mechanical properties is evaluated based on EBSD scans, texture analyses, stress-strain curves, and r-value measurements.

3.1. Crystallographic texture evaluation

Microstructure images of AA5182-O (as-received), CBT processing (CBT only), and CBT processing and recovery heat treatment (recovery HT) samples are obtained from EBSD scanning. CBT processing is applied along the RD. The RD-ND plane of the samples are scanned as shown in Fig. 4. As is evident, the quality of scans is low after CBT processing because of severe straining and underlying defects, which distort Kikuchi patterns used in image creation.

Grain configurations of CBT only and recovery HT show similar size and shape elongated along the CBT processing direction, while the initial state observed in the as-received condition is more equiaxed. This indicates that the material is subjected to a severe, biased deformation during CBT processing. In addition, the material is seen to be recovered by the imposed heat treatment condition without grain recrystallization.

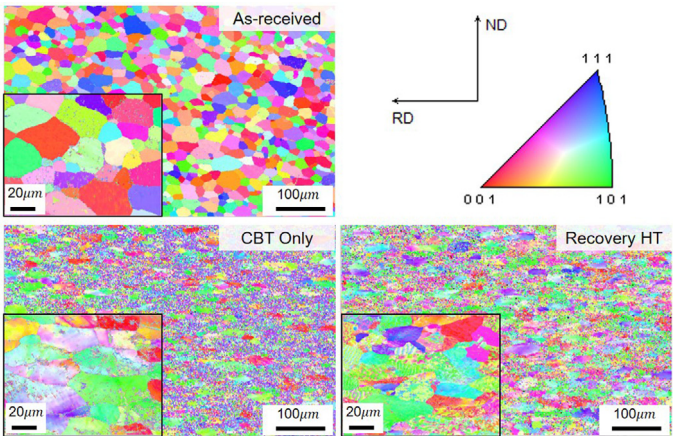

Fig. 4. EBSD images for (a) as-received, (b) CBT only, and (c) recovery heat treatment conditions. CBT processing only in the RD for EBSD.

The corresponding pole figures of each condition are shown in Fig. 5. Note that the figures (a–c) are the experimental measurements and (d) is the simulation (discussed in the next section). As-received condition shows a weak <001> cubic texture with low intensity, but through CBT processing, the material develops a moderate <111> texture. The simulated CBT texture shows a

Please cite this article as: J. Ha et al., Inducing <111> texture in AA5182-O through continuous-bending-under-tension and recovery heat treatment processes to influence
?r-values, CIRP Annals - Manufacturing Technology (2022), https://doi.org/10.1016/j.cirp.2022.04.059

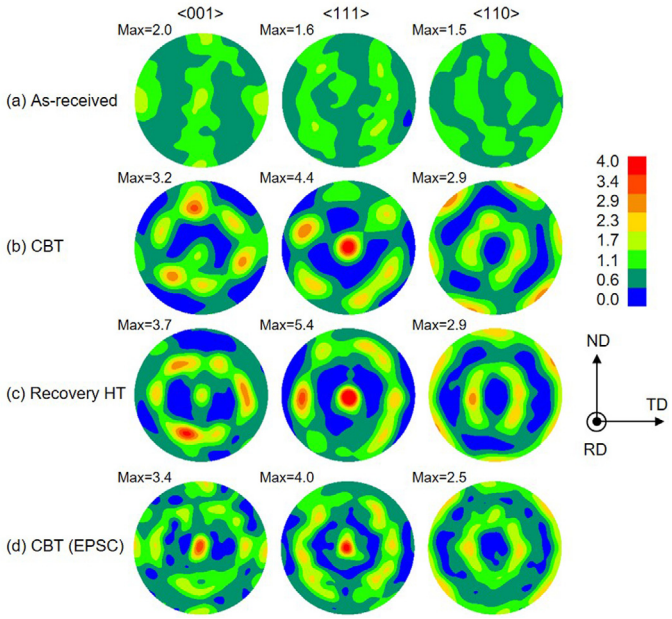

Fig. 5. Pole figures for (a) as-received, (b) CBT only, (c) recovery HT (experiment), and (d) simulated RD tension as approximation to CBT conditions. CBT processing only in the RD for EBSD.

similar result, with the maximum <111> intensity slightly lower than the experiments. This texture is preserved through the recovery heat treatment.

3.2. Stress-strain response

Fig. 6 represents an undeformed CBT specimen with 1x, 2x, and 3x bending-unbending cycles per stroke, based on the number of rollers that interact with the material at the specific location along the gauge section [13]. From the 3x region, where the most stress superposition effect occurs, a ASTM E8 subsize specimen is extracted for uniaxial tension testing after the CBT processing and recovery HT. Three orientations, RD, 45°, and TD, are examined for each condition. The obtained engineering stress-strain curves are shown in Fig. 7. Note that the AA5182-O sheet exhibits the Portevin-Le Chatelier effect, which results in the serrated flow in the stress-strain curves and the non-uniform deformation. Thus, the stress and strain quantities in Fig. 7 are calculated assuming uniform deformation.

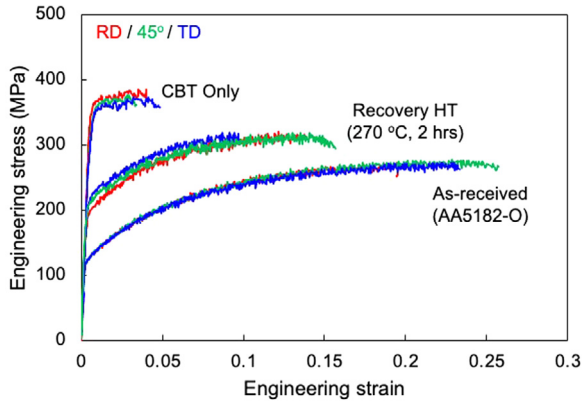

Fig. 6. Strip CBT specimen with three rollers and the 1x, 2x, and 3x deformation regions based on the number of bending-unbending cycles per stroke and ASTM E8 subsize specimen.

Flow stresses are increased by work hardening during the CBT processing, and then reduced by the recovery HT with a corresponding increase in the ductility. With the results observed in EBSD and pole figures, the heat treatment successfully recovers the microstructure enough to reduce the residual stress and regain moderate ductility for a subsequent forming process while the enhanced <111> texture obtained in the CBT processing is well maintained. An anisotropic material orientation effect is not strongly observed in the stress-strain curves.

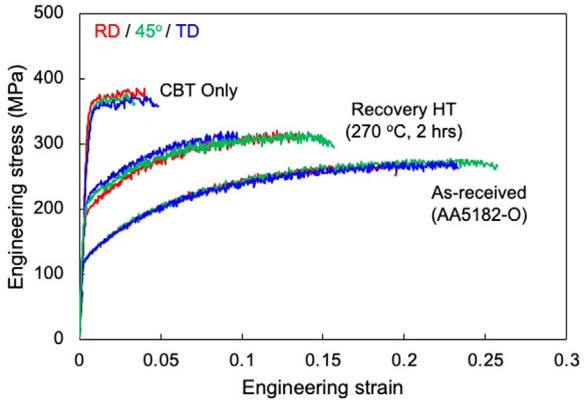

Fig. 7. Engineering stress-strain for as-received, CBT only, and recovery HT conditions in three sheet orientations.

3.3. r-values

Along with the stress-strain responses, the effect on r-values in the three orientations is investigated with respect to the plastic anisotropy in the strain during uniaxial tension (see Fig. 8). Two dimensional digital imaging correlation (2D-DIC) is used to measure the surface strain field. The DIC parameters are 29 pixels, 7 pixels, and 9 for the subset, step, and filter sizes, respectively. Assuming the uniform deformation, r-value is determined at five locations along the gauge section and the average value is taken for a constant r-value. Although the effect of CBT processing and recovery HT shown in the r-values is not as significant as in the stress-strain curves, a desirable result obtained is that the r-value variation between the three orientations, so called planar anisotropy, decreases. This could reduce the potential additional processes related to the planar anisotropy in a forming process, such as trimming an uneven cup wall, i.e., earing, in a deep drawing. Note however that the slight decrease in r-value with CBT process is not desirable with respect to formability.

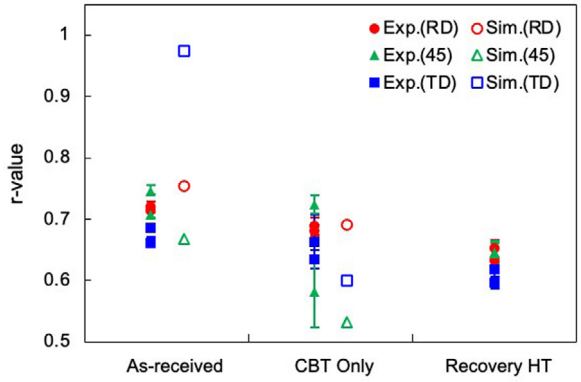

Fig. 8. r-values for two specimens in as-received, CBT only, and recovery HT conditions in three sheet orientations.

4. Numerical validation

In this section, the measured uniaxial tension data is modeled using an elasto-plastic self-consistent (EPSC) crystal plasticity model and the RD tension texture results are used to compare with measured CBT textures.

4.1. EPSC model

The EPSC model developed for AA6022-T4 [15] is adapted here for modeling of AA5182-O. In EPSC modeling, the polycrystalline material is described with a set of weighted orientations and each one is modeled as an ellipsoidal single crystal grain where the Jaumann rate of stress, $\hat{\boldsymbol{\sigma}}^c$, is calculated given the strain rate, $\dot{\boldsymbol{\varepsilon}}^c$, for each crystal, c:

$$\hat{\boldsymbol{\sigma}}^c = \mathbf{C}^c\left(\dot{\boldsymbol{\varepsilon}}^c - \dot{\boldsymbol{\varepsilon}}^{pl,c}\right) - \boldsymbol{\sigma}^c tr(\dot{\boldsymbol{\varepsilon}}^c) \quad (1)$$

where $\mathbf{C}^c$ and $\dot{\boldsymbol{\varepsilon}}^{pl,c}$ are the single crystal stiffness tensor and the plastic strain rate, respectively. Each grain is treated as an elasto-plastic inclusion in a homogeneous equivalent medium (HEM) that represents the average properties of all other grains in the material. The self-consistent scheme then determines the polycrystalline

Please cite this article as: J. Ha et al., Inducing <111> texture in AA5182-O through continuous-bending-under-tension and recovery heat treatment processes to influence
?r-values, CIRP Annals - Manufacturing Technology (2022), https://doi.org/10.1016/j.cirp.2022.04.059

macroscopic response from the interaction between the HEM and the inclusions. Complete details of the dislocation-based crystal plasticity and latent hardening formulations implemented in EPSC can be found in [15].

4.2. Numerical simulation results

The EPSC model simulates a uniaxial tension process using the adjusted parameters for AA5182-O shown in Tables 1 and 2:

Table 1
Dislocation hardening model fitting parameters.

τ_0[MPa]	k_1 [m^{-1}]	g
28	1.5×10^8	0.028

Table 2
Latent hardening interaction matrix constants.

a_0	a_1	a_2	a_3	a_4	a_5
0.068	0.068	0.0454	0.625	0.137	0.122

The latent hardening interaction matrix constants are adapted from [16] for octahedral slip systems for FCC metals. The constants governing minor anisotropy represent self-, coplanar, Hirth, collinear, Glissile, and Lomer interactions.

The RD, 45°, and TD uniaxial tension experiments are simulated to match the measured data at about 0.25 strain. Deformed texture of simulation shown in Fig. 5 is modeled with a uniaxial tension in the RD to 0.42 strain. The figures show reasonable agreement with the measured CBT texture intensities. However, the measured pole figures contain peak patterns not visible in simulated results, suggesting some minor effect of the superimposed bending, which is not modeled in EPSC. The simulated r-values from the initial and deformed CBT textures are shown in Fig. 8. The r-values for the simulated initial and deformed textures show good agreement with measured values, including the decreasing r-value trend. Despite the fact that the predicted r-value in TD deviates from measured value, Fig. 9 shows excellent approximation of the uniaxial tension responses in the RD, 45°, and TD directions.

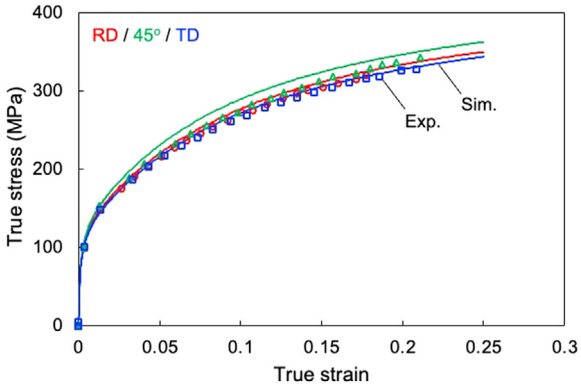

Fig. 9. Experiment (symbol) and simulation (solid line) stress-strain curves for uniaxial tension in the RD (red, circle), 45° (green, triangle), and TD (blue, square) for the as-received specimen.

5. Conclusions and outlook

Sequential processing by CBT and recovery HT allows for the successful regaining of ductility at high strength while the texture is preserved. EBSD images and pole figures confirms the texture of <111> fiber is enhanced through the stress superposition of continuous bending and tension. Numerical simulations using EPSC show a good agreement with the measured pole figures in the experiments. Regarding the resulting mechanical properties of the predicted texture, the stress-strain responses in the three orientations match well while the r-values are relatively less accurate. Still, the good accuracy on the texture development is promising as the numerical simulations could be used to determine the desired processing sequence and to achieve desired mechanical properties, i.e., r-values, to improve formability.

Declaration of Competing Interest

The authors declare that they have no known competing financial interests or personal relationships that could have appeared to influence the work reported in this paper

Acknowledgments

Funding for the NH BioMade Project from the U.S. National Science Foundation EPSCoR award (#1757371) and an AA5182-O material donation from Novelis are gratefully acknowledged.

References

[1] Singh RK, Singh AK, Prasad NE (2000) Texture and Mechanical Property Anisotropy in an Al-Mg-Si-Cu Alloy. *Materials Science and Engineering A* 277(1–2). 114-12.
[2] Jiang L, Jonas JJ, Mishra RK, Luo AA, Sachdev AK, Godet S (2007) Twinning and Texture Development in Two Mg Alloys Subjected to Loading Along Three Different strain Paths. *Acta Materialia* 55(11):3899–3910.
[3] Srinivasan N, Velmurugan R, Singh SK, Pant B, Kumar R (2020) *Materials Characterization* 164:110349.
[4] Meyer M, Kienzle O (1962) Verfahren zur Erzielung Glatter Schnittlinien. *CIRP Annals* 2:111–116. XI/.
[5] Tekkaya AE, Groche P, Kinsey BL, Wang ZG (2023) Plasticity and Future Opportunities of Stress Superposition in Metal Forming. *CIRP Annals* . STC-F Keynote (in preparation).
[6] Roskosz S, Chrapoński J, Madej Ł (2021) Application of Systematic Scanning and Variance Analysis Method to Evaluation of Pores Arrangement in Sintered Steel. *Journal of the International Measurement Confederation* : 168.
[7] Felde A, Rudolf S, Liewald M (2009) Enhancement of Process Limits in Cold Extrusion. In: *Proceedings of the International Conference on "New Developments in Forging Technology"*, 293–309.
[8] Maaß F, Hahn M, Tekkaya AE (2021) Adjusting Residual Stresses by Flexible Stress Superposition in Incremental Sheet Metal Forming. *Archive of Applied Mechanics* .
[9] Emmens WC, van den Boogaard AH (2009) Incremental Forming by Continuous Bending Under Tension—An Experimental Investigation. *Journal of Materials Processing Technology* 14:5456–5463. 209/.
[10] Poulin CM, Korkolis YP, Kinsey BL, Knezevic M (2019) Over Five-Times Improved Elongation-to-Fracture of Dual-Phase 1180 Steel by Continuous-Bending-Under-Tension. *Materials and Design* 161:95–105.
[11] Poulin CM, Vogel SC, Korkolis YP, Kinsey BL, Knezevic M (2020) Experimental Studies into the Role of Cyclic Bending During Stretching. *International Journal of Material Forming* . https://doi.org/10.1007/s12289-019-01530-2.
[12] Zecevic M, Roemer TJ, Knezevic M, Korkolis YP, Kinsey BL (2016) Texture Evolution in Continuous-Bending-under-Tension of Al 6022. *Materials* 9:130–144.
[13] Roemer TJ, Barrett TJ, Knezevic M, Kinsey BL, Korkolis YP (2019) Experimental Study of Continuous-Bending-Under-Tension of AA6022-T4. *Journal of Materials Processing Technology* . https://doi.org/10.1016/j.jmatprotec.2018.11.046.
[14] Ha J, Piccininni A, Korkolis YP, Palumbo G, Knezevic M, Kinsey BL (2021) Formability Improvements of AA5754-H32 at Room Temperature via Continuous Bending Under Tension (CBT) and Pre-forming Heat Treatment. *Forming the Future*, 1805–1812.
[15] Feng Z, Yoon S, Choi J, Barrett TJ, Zecevic M, Barlat F, Knezevic M (2020) A comparative study between elasto-plastic self-consistent crystal plasticity and anisotropic yield function with distortional hardening formulations for sheet metal forming. *Mechanics of Materials* 148:103422.
[16] Ghorbanpour S, Zecevic M, Kumar A, Jahedi M, Bicknell J, Jorgensen L, Beyerlein IJ, Knezevic M (2017) A Crystal Plasticity Model Incorporating the Effects of Precipitates in Superalloys: Application to Tensile, Compressive, and Cyclic Deformation of Inconel 718. *International Journal of Plasticity* 99:162–185.